This project is part of the PRIMA Programme supported by the European Union

RESERVOIR

Sustainable groundwater RESources managEment by integrating eaRth observation deriVed monitoring and flOw modelIng Results

PRIMA

GA no. 1924

DELIVERABLE D6.1

3D static model developed for the study sites

Author(s):	UNIPD: Yueting Li, Pietro Teatini, Claudia Zoccarato
Responsible Partner:	UNIPD
Version:	V1
Date:	31/08/22
Distribution Level (CO, PU)	PU

Acknowledgement

This project has received funding from the Partnership for Research and Innovation in the Mediterranean Area under the European Union's Horizon 2020 research and innovation programme under grant agreement No 1924.

Statement of originality

This document contains original unpublished work except where clearly indicated otherwise. Acknowledgement of previously published material and of the work of others has been made through appropriate citation, quotation or both.

* PU = Public; CO = Confidential, only for members of the consortium EU-R/R-UE = Classified, as referred to in Commission Decision 2001/844/EC.

DOCUMENT REVISION HISTORY

Date	Version	Editor	Comments	Status
31/08/2022	1.0	Yueting Li, Pietro Teatini, Claudia Zoccarato (UNIPD)		1st ver.
31/08/2022	1.0	Claudia Meisina (UNIPV)		1st ver.
31/08/2022	1.0	Carolina Guardiola (IGME)		1st ver.
31/08/2022	1.0	Roberto Tomás (UA)		1st ver.
31/08/2022	1.0	Khaldoun Shatanawi (UJ)		1st ver.
31/08/2022	1.0	Ali Hakan Oren (DEU)		1st ver.

LIST OF PARTNERS

Participant	Name	Country
UNIPV	Università degli studi di Pavia	Italy
UNIPD	Università di Padova	Italy
IGME	Instituto Geológico y Minero de España	Spain
UA	Universidad de Alicante	Spain
DEU	Dokuz Eylul University	Turkey
UJ	The University of Jordan	Jordan
CER	Consorzio di Bonifica di secondo grado per il Canale Emiliano Romagnolo	Italy
RSCN-AWR	Royal Society for the Conservation of Nature - Azraq Wetland Reserve	Jordan

GLOSSARY

Acronym	Description
InSAR	Interferometric Synthetic Aperture Radar
EO	Earth Observation
DA	Data Assimilation
PDF	Probability Density Function

FEM	Finite Element Method
SM	Static models
PO	Project Objectives
WP	Work Package

ABSTRACT

This deliverable corresponds to the task *T6.1 – 3D static model developed for the study sites* included in WP6 (Deformation Model Development). It presents the first phase of the geomechanical modelling framework aimed at simulating the process of land subsidence caused by pore pressure depletion and characterizing the storage properties of the exploited aquifer systems. At this stage, the conceptual models produced in WP2 and the geological information collected in WP5 are integrated to build the so-called *static models (SM)*. SM refers to the construction of the finite element meshes based on geological data to be used for the simulation of the dynamic processes of land deformation due to the aquifer exploitation. The pilot sites of Alto Guadalentín aquifer (AG, Spain), Gediz River Basin (GRB, Turkey) and Azraq Basin (AB, Jordan) are considered in this task. The lack of significant land subsidence in the Comacchio plain, Italy, as revealed by InSAR measurements acquired in WP3, suggested to focus the modelling activities on the process of saltwater intrusion in the coastal aquifers of this pilot site and the possible management strategies of this process strongly impacting the coastland rather than on geomechanical issues.

CONTENTS

LIST OF FIGURES

INTRODUCTION, GOAL AND PURPOSE OF THIS DOCUMENT

The aim of RESERVOIR project is to provide new products and services for a sustainable groundwater management model to be developed and tested in four water-stressed Mediterranean pilot sites and then be applicable in other regions via an interdisciplinary approach.

The specific Project Objectives (PO) are the following:

- PO1. Develop an innovative methodology for the hydrogeological characterization of large-scale aquifer systems using low-cost and non-intrusive data such as satellite-based Earth Observation (EO) techniques.
- PO2. Integrate advanced EO techniques into numerical groundwater flow and geomechanical models to improve the knowledge about the current capacity to store water and the future response of aquifer systems to natural and human-induced stresses.
- PO3. Enhance the knowledge about the impacts of agricultural and tourism activities on the water resources by quantifying the ground deformation during the monitored periods.
- PO4. Engage water management authorities and provide models for an optimal management of the aquifer systems. We will engage 4 water authorities in 4 different countries through a series of face-to-face workshops (each participant will organize at least 1 workshop in the first 4 months of the project). The water authorities will be involved in the conceptualization and design of guidelines for Groundwater Resource Management. Best practices of water management for agricultural and tourism purposes will be developed taking advantage of the knowledge and methodologies from the outputs of PO1, PO2 and PO3.
- PO5. Dissemination and exchange of the generated knowledge among the experts and the managers in charge of land and groundwater management in the pilot sites to strengthen the aquifer resilience.

Work package WP6 (with WP5) aims at integrating advanced Earth Observation (EO) techniques into numerical geomechanical (and groundwater flow) models to improve our knowledge about the capacity of aquifers to store water and predict the future response of aquifer systems to stresses (PO2).

Geomechanical models have been widely used to simulate land subsidence caused by aquifer overexploitation. The removal of groundwater from the subsurface causes the pore pressure to decline within the pumped aquifer system. The geostatic load, less supported by the pore fluids, becomes more sustained by the grain-to-grain contacts (Terzaghi 1923). The increase of the so-called "effective intergranular stress" $\Delta\sigma_z$, which is equal to the pore pressure decline Δp, yields the porous medium to compact and the land surface to subside. Soil compaction η, and therefore land subsidence, directly depend on soil compressibility C_m. In the simplest condition of one-dimensional (vertical) deformation, it can be written (Gambolati and Teatini 2015):

$$\eta = C_m \, \Delta\sigma_z \, s$$

with s the thickness of the depleted aquifer. The same compressibility parameter also characterizes the capability of an aquifer to store (or release) water. In fact, the specific elastic storage S_s and C_m are related through the well-known relationship (Gambolati and Teatini 2015):

$$S_s = \gamma_w (C_m + \phi\beta)$$

where γ_w and β are the specific weight and volumetric compressibility of the water, and ϕ the aquifer porosity.

The accuracy of numerical modelling of land subsidence and characterizing aquifer storage is highly dependent on the knowledge of key geomechanical properties like soil compressibility (C_m). Generally, there is limited in-situ information to attain a credible characterization of C_m. WP6 is aimed at providing a methodology to characterize C_m by optimizing numerical results taking advantage of Earth Observations of land subsidence in the selected pilot sites. This methodology, also known as inverse modelling, can be implemented by Bayesian-based methods. It is worth noting that in a Bayesian scheme, compressibility C_m is characterized by a probability density function (PDF) rather than a deterministic value. In other words, this study aims to reduce the uncertainties of compressibility C_m which can improve the numerical model performance on predicting the aquifer responses to groundwater exploitation.

Specifically, WP6 is subdivided in four tasks:

- T6.1 – Static modelling
- T6.2 – Fluid-dynamic modelling
- T6.3 – Geomechanical modelling
- T6.4 – Modelling scenarios

In task 6.1 (this deliverable) the conceptual geological model of the pilot sites derived in WP2, the results of the engineering-geological characterisation and interpretation carried out in WP4, and the grids developed to simulate the pressure evolution in the study aquifer systems (WP5) are used to develop a 3D static model (SM). The 3D domain is discretised in (tetrahedral or hexahedral) finite elements. Mesh density is properly chosen to represent in detail the complexity of the geological sequences and the distribution of the main stressors (wells). In this derivable, the details of the 3D SMs for three pilot sites, namely the Alto Guadalentín aquifer (Spain), the Gediz River Basin (Turkey) and the Azraq Basin (Jordan), are presented. The SMs are developed based on the corresponding conceptual models described in previous Deliverables 2.4 and 5.4. Due to the absence of significant land displacements, as revealed by the WP3 outcomes, the Comacchio pilot site will be investigated from the groundwater quality point of view, specifically in relation to the process of saltwater intrusion in the shallow coastal aquifer system.

Two different approaches are used to build the 3D SMs according to data availability and site-specific characteristics of the pilot sites. A one-way coupled approach (Teatini et al. 2006; Bonì et al. 2020) for the pilot sites in Turkey and Jordan. The workflow consists of taking advantages of the groundwater flow grids developed in WP5 and use the calibrated hydraulic head changes as input for the geomechanical models. Thus, in these cases, the geomechanical grids are taken from the groundwater flow grids and adapted to assign appropriated boundary conditions for the geomechanical simulations. The approach differs in the case of the aquifer in Spain. Due to the large lowering (more than 100 m) of the water table because of groundwater pumping, the effect of the water content changes on the geomechanical response of the system must be properly considered. This requires the use of a fully coupled, variably saturated groundwater flow and geomechanical model (Nardean et al. 2021). Therefore, the mesh of the Alto Guadalentín aquifer system is built from scratch using all the available geological and hydrological information made available by the previous WPs.

The methodology implemented and the static modelling outcome are explicated in the corresponding sections for each pilot site. Notice that some modifications with respect to the previous grids developed in

WP5 were introduced according to the characteristics of the boundary conditions needed by the three-dimensional geomechanical models.

1 The Alto Guadalentín Basin, Spain

1.1 Available geological information

The Alto Guadalentín Basin is located in Southeast Spain, which covers an area of 250 km^2. The basin is NW-SE oriented and is mainly surrounded by outcropping Miocene and Triassic fillings. The northwest of the basin is hydraulically connected to the Bajo Guadalentín Basin (Bonì et al. 2015). The local aquifer system overlies a Paleozoic pre-orogenic metamorphic basement with horst and graben patterns. The thickness of basement varies from 300 to 900 m. Plio-Quaternary and Miocene sediments constitute the aquifer from top to bottom. Furthermore, the Pilo-Quaternary filling can be divided into two sublayers in the central part of the basin: i) the upper layer is composed of clay, which contributes largely to land subsidence; and ii) the lower one mainly consists of sand with embedded silt matrix. This sand layer is the main productive unit. Miocene filling is composed by conglomerates, marls and sandstones and regarded as an almost impervious unit (Cerón García 1995).

1.1.1 The isobath maps

As aforementioned, the aquifer system is composed of Plio-Quaternary and Miocene materials. Moreover, Plio-Quaternary can be subdivided into a clay layer and a sand layer while Miocene materials can be regarded as one layer since it is impervious and stiff.

The isobath map of clay thickness is retrieved from previous work by Béjar-Pizarro et al. (2016) (Figure 1-1(a)), while the isobath maps of Plio-Quaternary filling and Miocene filling are estimated by Cerón García (1995) (Figure 1-1(b)). Regarding Miocene materials, the actual thickness variability is more complicated than that showing in Figure 1-1(c) and used in the model. In fact, the thickness of Miocene filling is larger than 600 m in certain areas and it is intercepted by several faults which causes abrupt offsets. We miss out most of these discontinuities because the Miocene filling contributes little to discharge and land subsidence.

1.2 Static model

The groundwater water flow model published by Ezquerro et al. (2017) accounts for the Plio-Quaternary and Miocene sediments, with the latter layer regarded as the zero-flow boundary. In 3D geomechanical modelling, zero-displacements boundary conditions need to be imposed sufficiently far from the area where the pore pressure varies and the displacements occur. For this reason, the model domain has been extended with respect to the domain in Ezquerro et al. (2017), also including the bedrock basement and the hills surrounding the alluvial plain (Figure 1-1(d)). Furthermore, the previous study area was bounded to the northeast by an administrative border dividing the Alto and Bajo Guadalentín aquifers (Figure 1-1(d)). Based on the displacement contour map derived by InSAR data (Bonì et al. 2015) and provided by WP3, large land subsidence was measured in that area. Therefore, the model domain has been extended to the north-east where land subsidence is negligible. The new study area includes a small portion of Bajo Guadalentín Basin.

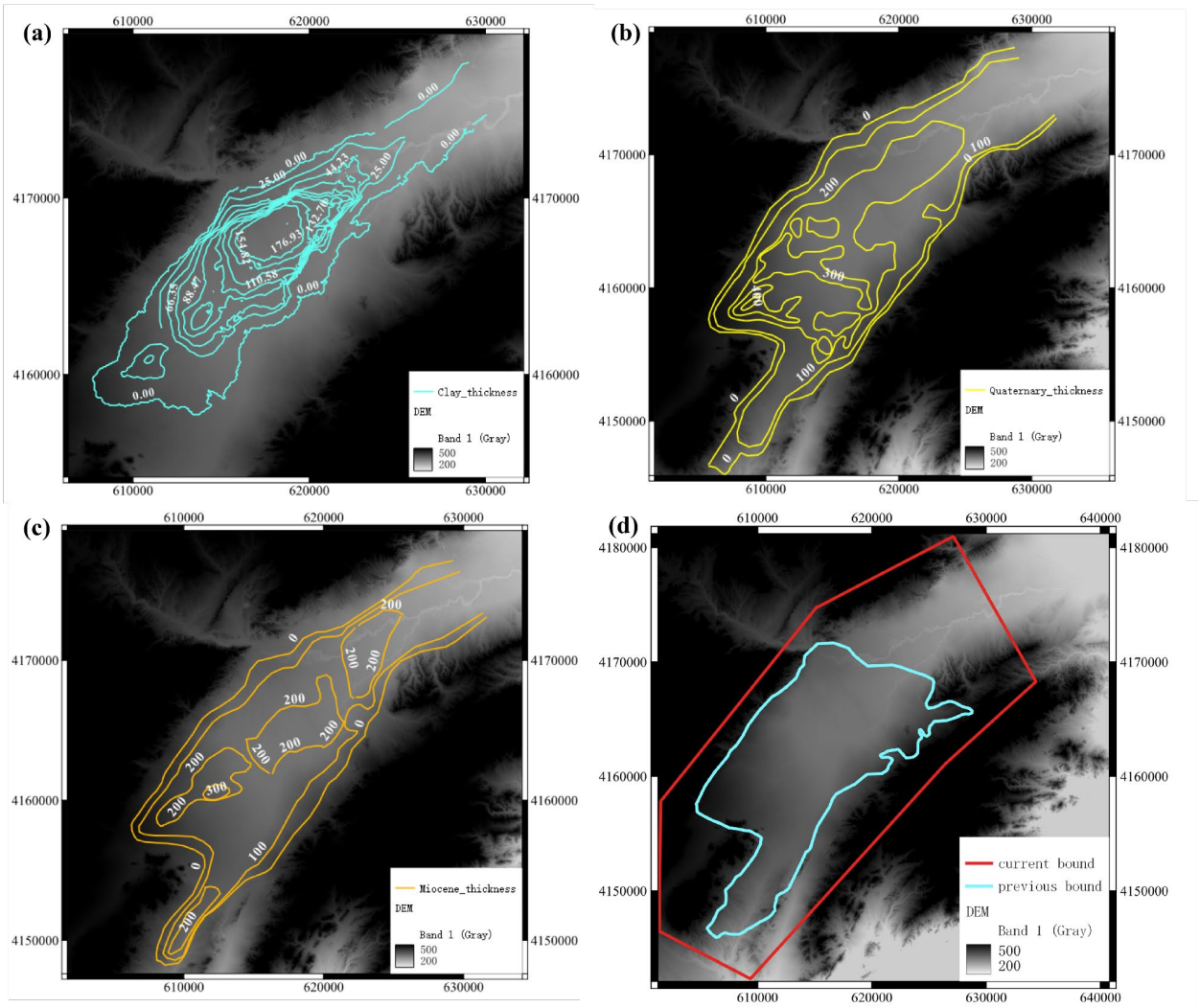

Figure 1-1 (a) Compressible clay thickness isobath (Ezquerro et al. 2017); (b) Plio-Quaternary filling isobath (Cerón García 1995); (c) Miocene filling isobath (Cerón García 1995); (d) comparison between the previous Alto Guadalentín model boundary domain (Ezquerro et al. 2017) and the current boundary domain. The background of all subplots is a raster image representing the digital elevation model (DEM) in m above mean sea level (amsl) of the study area.

1.2.1 Set up of the static model

After determining the domain area, the generation of the 3D SM can be subdivided into the following steps:

1) The study area is discretized into triangular elements as shown in Figure 1-2. The triangular discretization of 2D domain consists of 8,147 nodes and 15,939 elements. The representative size of the 2D elements is about 300 m, which is fine enough to depict the spatial variability of each layer and keep a trade-off between model accuracy and mesh size.

2) Generation of surfaces to characterize the top of each layer by imposing the corresponding z-coordinates at each node. Specifically, the elevation of the domain top is directly sampled from the raster image provided by IGME. It worth noting that the maximum elevation of the domain is set to 450 m amsl. There are two reasons for cutting the elevation of the hills surrounding the valley. First, they are useless for numerical simulation whereas the presence of these rock leads to more redundant nodes and elements. From a hydrological point view, they are attributed to unsaturated zone where the effective permeability is also a function of the elevation above the water table. The effective permeability begins to plunge at a certain

elevation. In the worst cases, the numerical simulation could crash due to this abrupt decrease of the effective permeability.

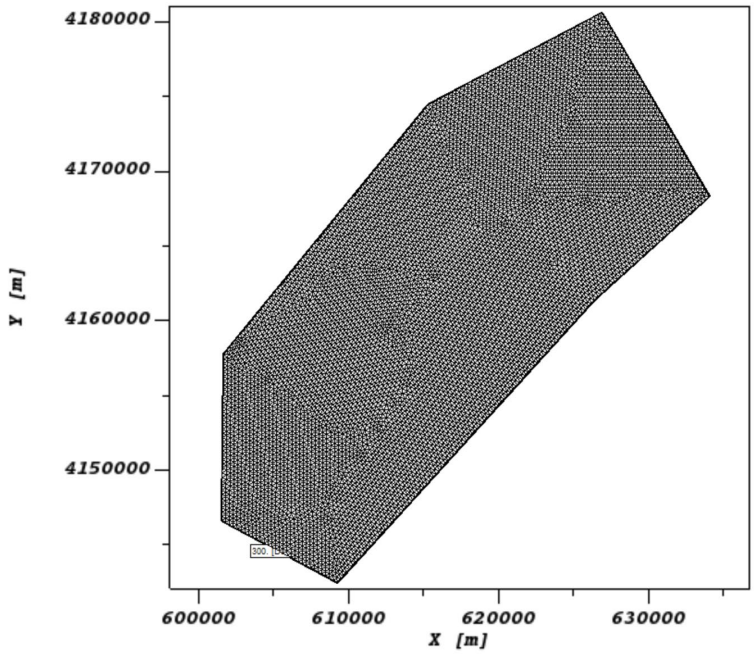

Figure 1-2 The triangular discretization of the 2D Alto Guentalentin domain, with 8,147 nodes and 15,939 elements.

3) Interpolation of the isobath map of clay and sample the clay thickness at each node from interpolation result. The elevation of the clay bottom is attained by subtracting its thickness from the top surface elevation. The same step is repeated for sand and Miocene layers. Note that the sand thickness is derived by subtracting the clay thickness from the Pilo-Quaternary sediment thickness. Besides, the top 50 m of Miocene unit is considered as an individual layer with possible relative higher permeability to allows water extraction, as suggested by IGME. The leftover part is regarded as an impervious boundary. The bottom of the domain is set to -350 m amsl, which guarantees the domain is bounded by the bedrock. In this step, the domain is divided into 5 geologic layers through 6 surfaces.

4) Building of the 3D grid by stacking all 6 surfaces and connecting them from top to bottom. With the aid of GEN3D (Teatini et al. 2006), we developed a 3D coarse mesh consisting of 104,993 tetrahedral elements and 25,844 nodes. However, the mesh needs to be further refined especially along vertical direction to model more precisely the variation of parameters such as the pressure head, saturation degree, and displacements.

5) Refining of the coarse mesh by means of TETGEN (Si 2015), a software that allows to assign unlike tetrahedral volumes to different regions. In the final mesh, clay layer is the most finely discretized, followed by the sand layer, Miocene, and the bedrock. The characterized element size varies from ten to hundreds of meters. This fine mesh is composed by 164,073 nodes and 915,005 tetrahedral elements (Figure 1-3).

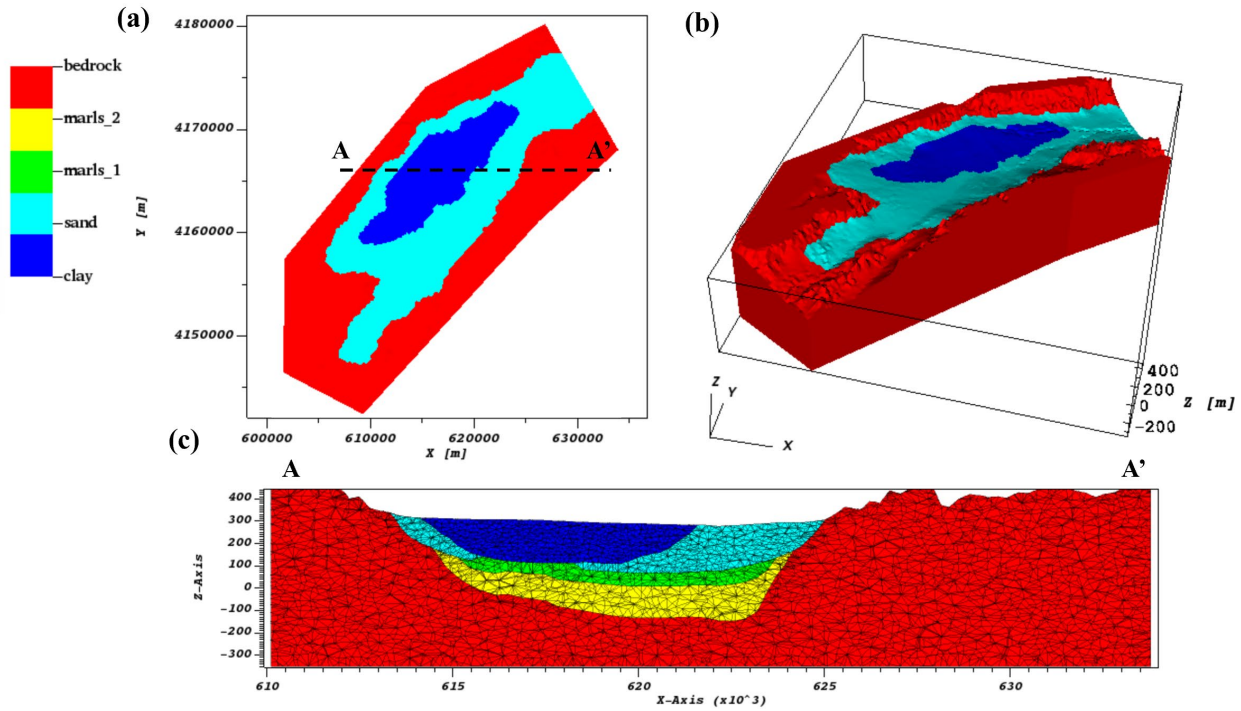

Figure 1-3 Domain of the updated static model in the Alto Guadalentín Basin. (a) Plan view of static model, with the profile AA' highlighted in black line; (b) Perspective view of 3D static model (Z-axis is exaggerated 10 times); (c) FE discretization along the AA' profile. The average element size in each geologic unit differs. The top and bottom of domain are set to 450 m and -350 m amsl, respectively.

1.2.2 Validation of the static model

In this paragraph the static model here developed is validated against the geological profiles after Cerón García (1995). Notice that the graphical representation of the geologic units differs in our and the Cerón García figures. The match between the two graphical representations, together with the traces of the vertical sections, are shown in Figure 1-4.

The comparison of the geologic setting along the vertical profiles are presented in Figure 1-5 and Figure 1-6. The figures show that the static model agrees with to the geological setting represented by Cerón García (1995), especially for the Plio-Quaternary fillings. The main differences occur for the marls layer, whose isobaths are simplified in our SM with respect to the previous work.

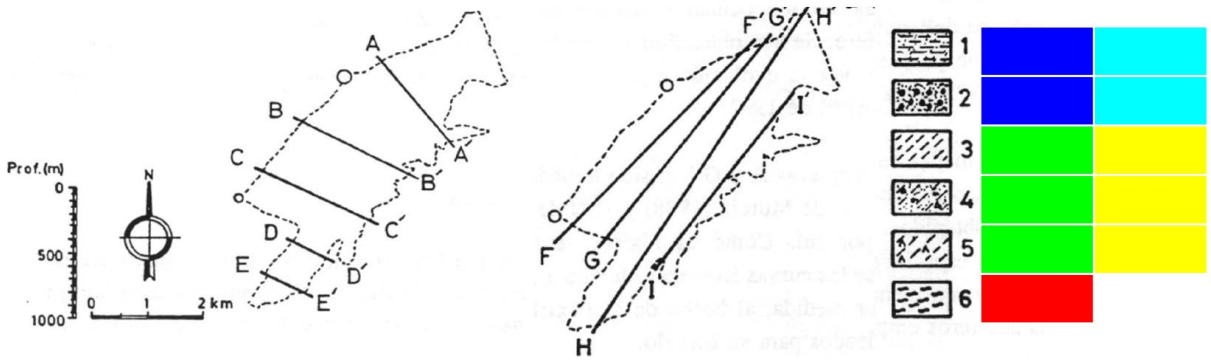

Figure 1-4 Transversal NW-SE and SW-NE geological profiles as published in Cerón García (1995). The soil classification is the following. 1: clays, limestone, sand and gravels; 2: sand, gravels and conglomerate; 3: marls; 4: marls with sand and conglomerate; 5: marls with gypsum; 6: metamorphic substratum. The correspondence between the legend of Cerón García (1995) and the one used in the SM build in this deliverable is shown to the right.

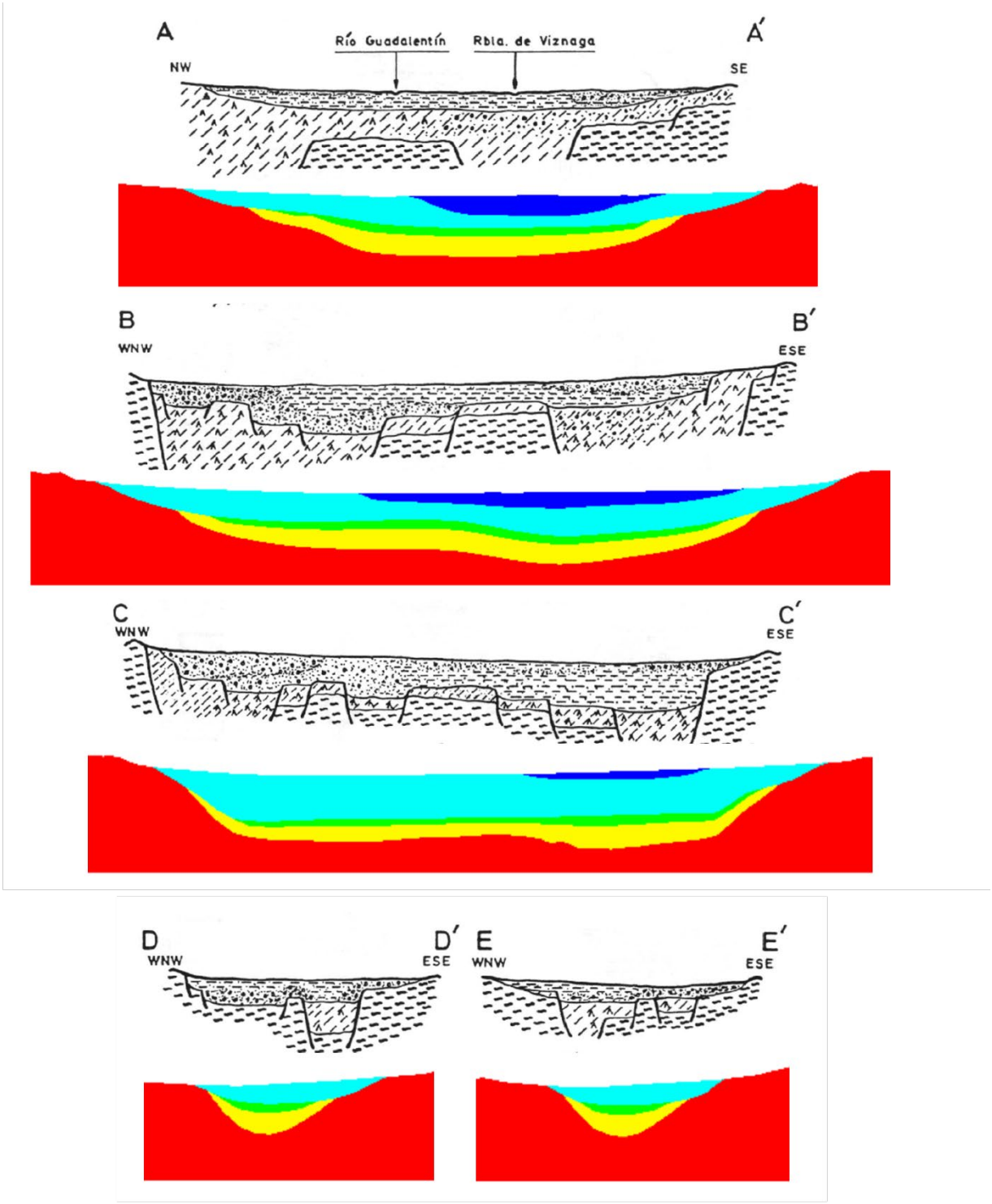

Figure 1-5 Comparison between the NW-SE geologic profiles as published in Cerón García (1995) and reconstructed in the SM of this deliverable.

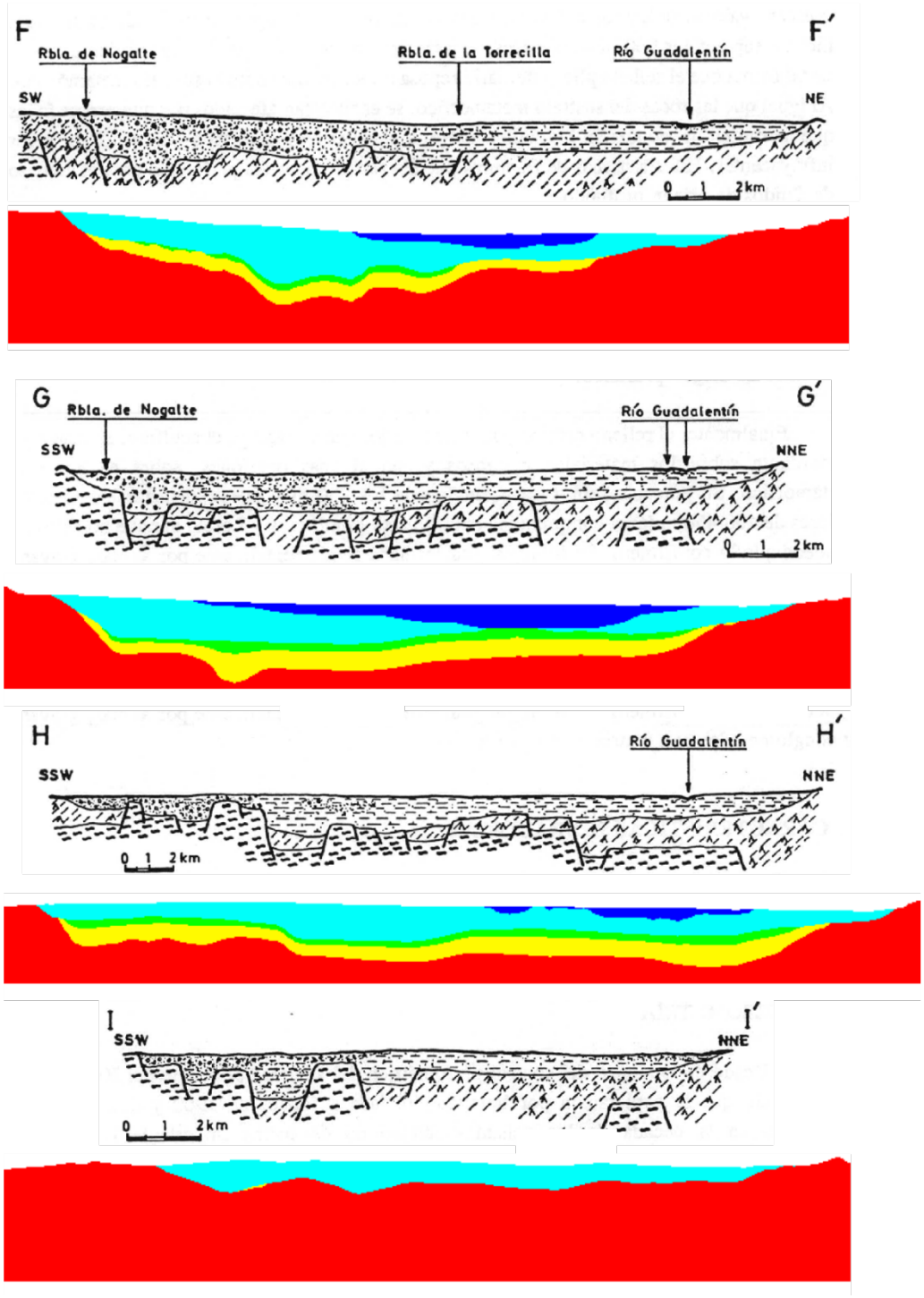

Figure 1-6 Comparison between the SW-NE geologic profiles as published in Cerón García (1995) and as reconstructed in the SM of this deliverable.

2 The Gediz River Basin, Turkey

2.1 Available geological information

The Gediz River Basin (GRB) is located in Turkey and covers a drainage area that amount to 17,034 km^2. The alluvial aquifer develops over the Gediz Graben which is WNW-ESE oriented (Sözbilir 2002). The selected

pilot site (Figure 2-1) is the eastern part of the alluvial aquifer of the GRB and covers an area of 431 km^2. This pilot site is bounded by hills except for the eastern border which connects to the westernmost part of the alluvial valley.

The aquifer system overlies a metamorphic basement and is made up of accumulated sedimentary materials. The bottom of the aquifer system is constituted by Neogene-aged, consolidated materials made by sandstone, conglomerate, claystone, limestone, and volcanic layers. The top of the formation is Quaternary alluvial deposits which are composed of clay, sand, and gravel (Seyitoglu et al. 2000).

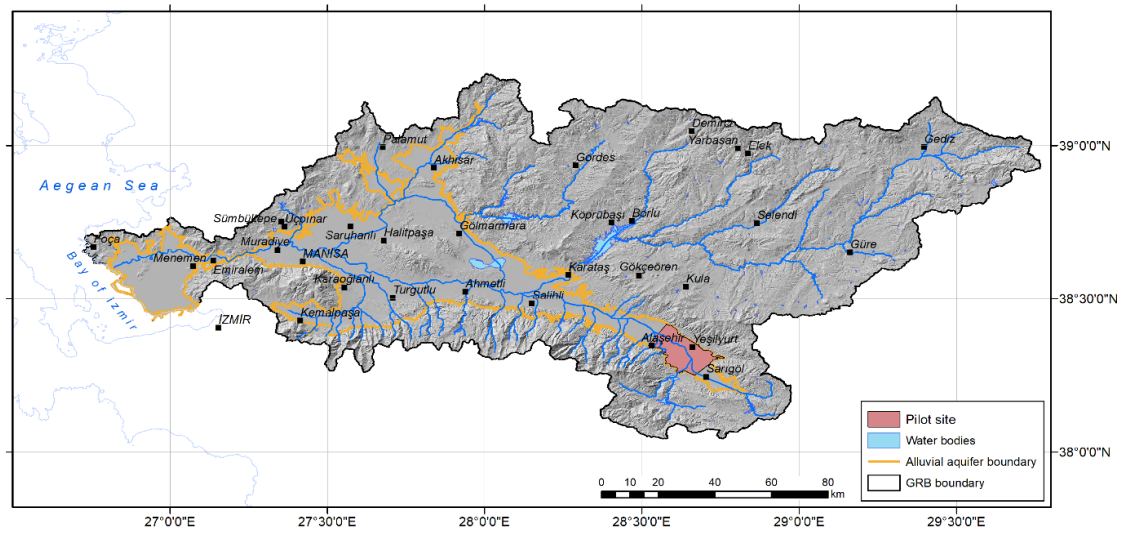

Figure 2-1 Location of the selected pilot site for the GRB alluvial aquifer.

2.1.1 The conceptual model of the GRB aquifer system

A conceptual model of the aquifer system has been established in Deliverable 2.4. The conceptual model consists of five layers (two clay and three gravel units) that represent different alluvial materials. The thickness of the various layers is shown in Figure 2-2. In general, these soils are poorly consolidated and may deform significantly if pore pressure declines.

Similarly to what has been presented for the previous pilot site, the development of a 3D geomechanical model requires the enlargement of the simulation domain (with respect to the strict aquifer system) in order to impose zero-displacement boundary conditions sufficiently far from the depleted (and consequently deforming) units. Therefore, the conceptual model needs to be extended to the consolidated layers (or rock basement) in the vertical direction. As for the horizontal extent, the pilot site is connected to the northwest and southeast with the remaining parts of the alluvial system. However, there is no difference about the hydraulic and mechanical properties between the pilot site and the remaining alluvial aquifer. For this reason, it is difficult to impose proper boundary conditions for both the groundwater flow and geomechanical models with the pilot site extension outlined in Figure 2-2. Consequently, the domain is enlarged in the horizontal direction too as it will be described in the next section.

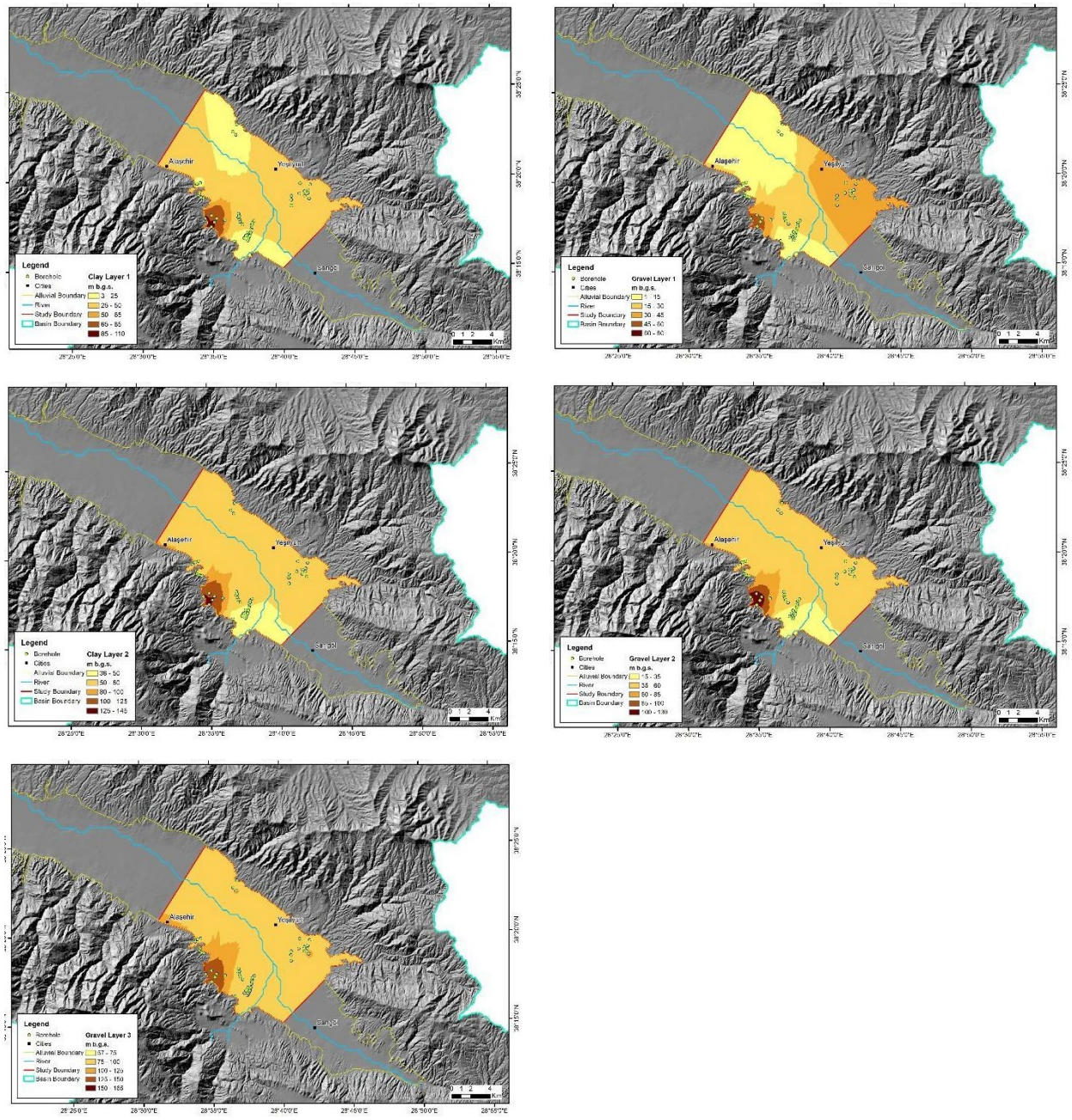

Figure 2-2 Contour maps showing the bottom depth of the five alluvial layers composing the GRB conceptual model.

2.1.2 The static model of groundwater flow

The horizontal area was updated by DEU, expanding the modelling domain as shown in Figure 2-3. The alluvial soils are largely bounded by hills that represent the inactive cells in Figure 2-3. The grid made for groundwater flow modelling was developed by DEU using ModelMuse (Winston 2019) and represents the five alluvial layers (Quaternary-aged layers). Each layer is discretized into 188 rows and 242 columns. The cell size is 150 m along both x (WE) and y (SN) directions. Overall, the grid is made of 227,480 cells, 70,088 of which are active.

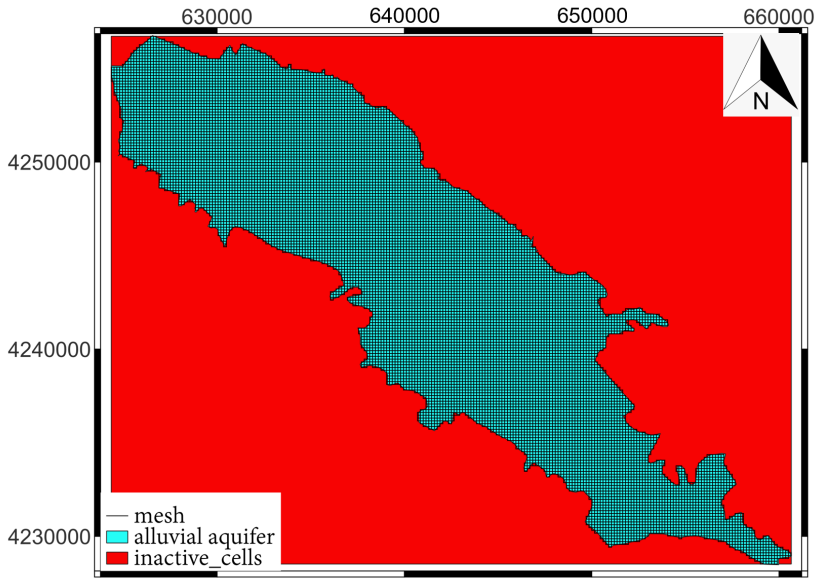

Figure 2-3 2D plan view of the GRB groundwater flow model. The discretization of the inactive cells is not shown for a clearer visualization of the alluvial aquifer.

Notice that ModelMuse uses a finite difference method (FDM) to solve the groundwater flow equation. On the other hand, the GEPS3D geomechanical simulator that will be used (Isotton et al. 2019) solves the equilibrium equations through a finite element method (FEM). GEPS3D uses hexahedral elements, whose topology and size have been properly derived from the FD grid to keep the same discretization. Therefore, no interpolation between the pressure field computed by ModelMuse and that in input to GEPS3D will be needed, thus keeping the solution accuracy. A specific driver converting the finite different grid into the equivalent hexahedral mesh has been developed.

2.2 Static model

2.2.1 Set up of the static model

As aforementioned, the SM for the geomechanical simulations needs to be updated by appending Neogene layer and the bedrock basement to the FD grid of the groundwater flow model as introduced in Section 2.1.2. To this aim, we should map the thickness variability of Neogene unit based on the available borehole logs. Unfortunately, the deep geothermal wells reaching this geologic unit are unevenly distributed in the study area (Figure 2-4). This makes impossible to derive a reasonable spatial distribution of Neogene unit from the available information. Therefore, this layer is simplified by assuming a constant thickness equal to 25 m. This value corresponds to the average of the thickness recorded in the drilling cores. Neogene materials are mainly composed by sandstone, conglomerate, claystone, limestone which makes this layer barely contributing to aquifer recharge and land subsidence. Like Miocene fillings in the Alto Guadalentín Basin, Neogene layer is designed to be a “transitional” part between the alluvial aquifer system and bedrock basement. The spatial variability of this layer will not significantly affect the modelling outcome. About bedrock, it ends at -100 m amsl. These two new appended layers follow the same horizontal discretization as the ModelMuse grid with 188 rows and 242 columns. Overall, the 3D SM is made of 7 geologic (and FE) layers, totaling 363,968 nodes and 315,469 hexahedra (Figure 2-5). Notice that the bedrock bounding the alluvial aquifer system laterally and at the bottom will be an “active” layer in the geomechanical computation, although characterized by a compressibility much smaller than that of the alluvial soils.

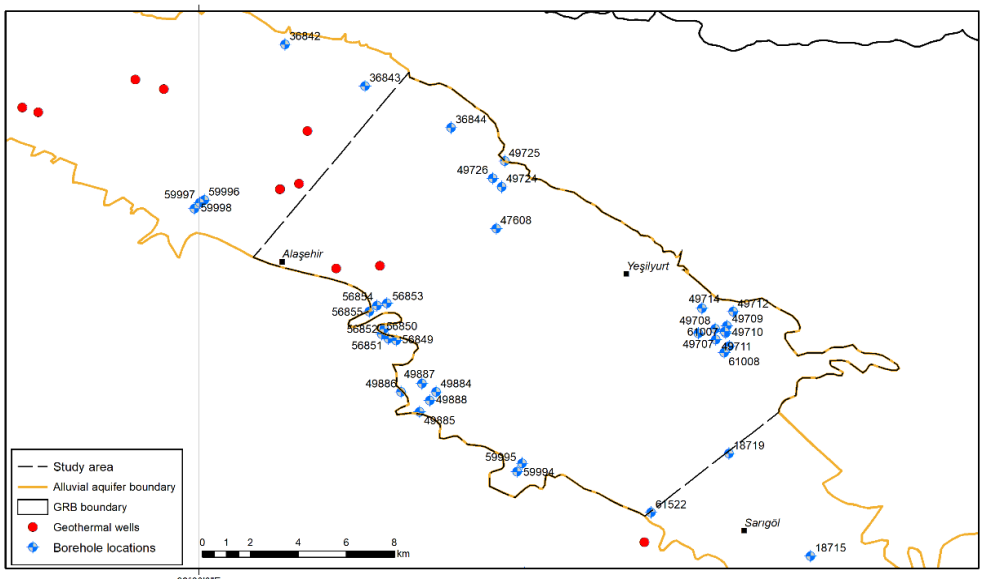

Figure 2-4 Locations of boreholes and deeper geothermal wells. The geothermal wells concentrate in northwest of the study area which makes it unfeasible to map the thickness variability of Neogene unit.

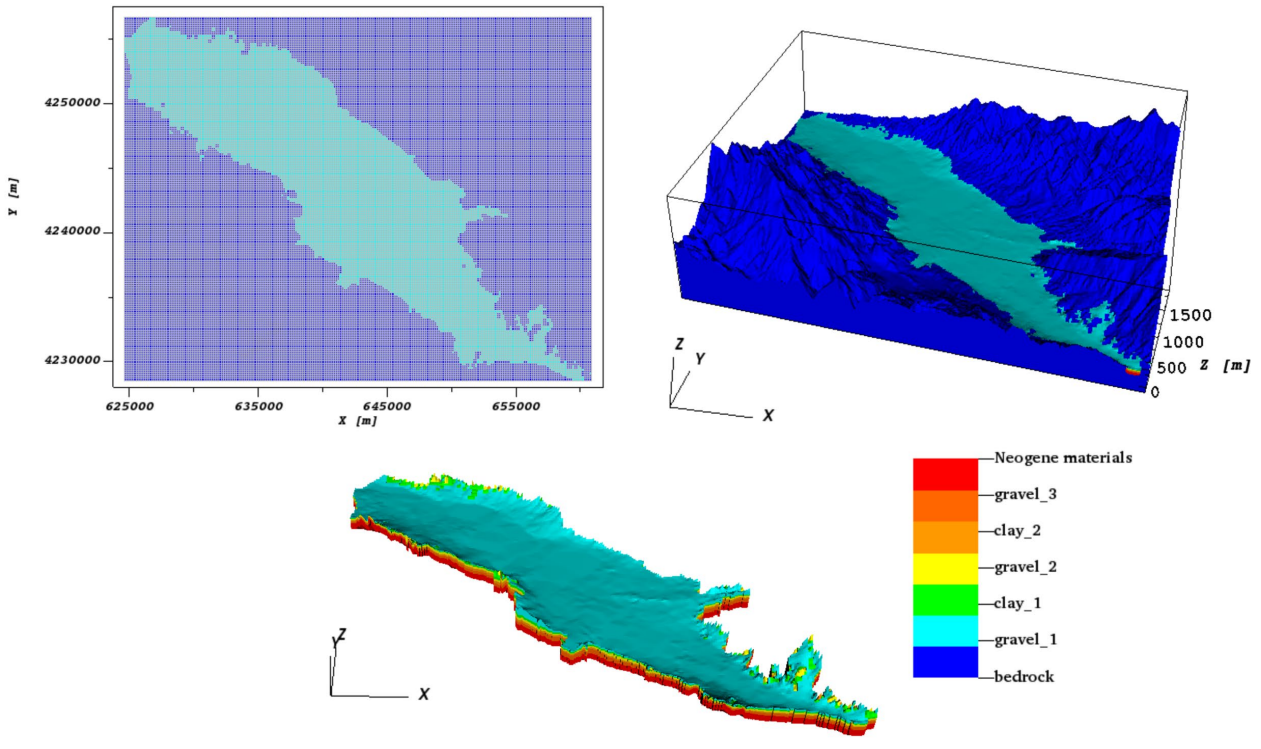

Figure 2-5 The domain of the updated static model for the GRB pilot site. (Top-left) The 2D plan view: (top-right) perspective view; and (bottom) the geologic layers excluding the bedrock.

2.2.2 Validation of the static model

Three SW-NE oriented profiles across the study area (Figure 2-6) have been reconstructed by DSI (2014). These profile sketches are compared with the corresponding cross-sections extracted from the SM. Figure 2-7 shows that the SM roughly depicts the trends of the alluvial aquifers but misses some details especially for the unconfined layers. For example, the spatial variation of these layers (gravel_1 and clay_1) are

simplified to regular shapes. Potential reasons for such simplifications include the low proportion accounting for their thickness and groundwater exploitation as well as the lack of geological information.

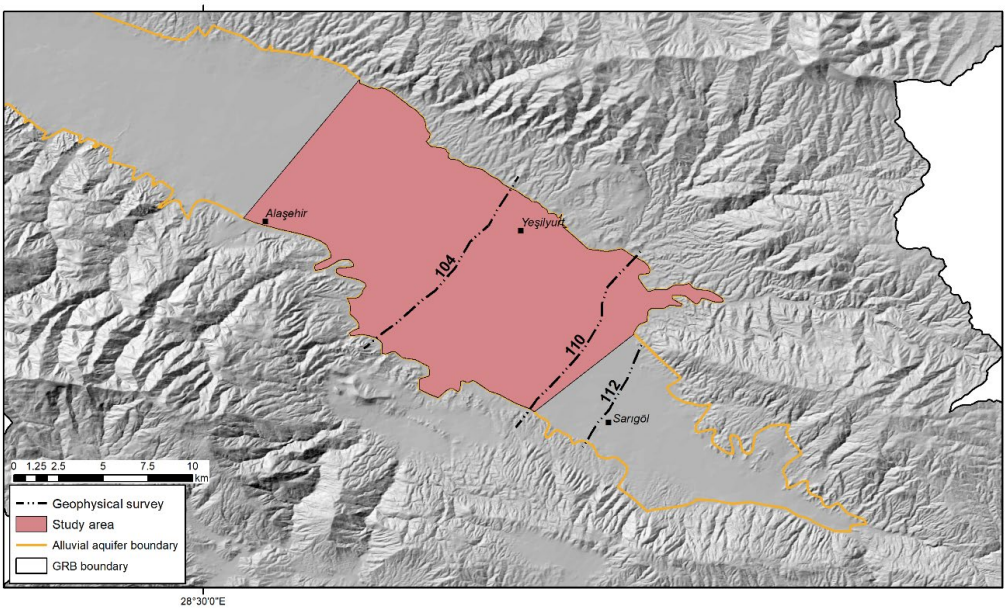

Figure 2-6 Geophysical survey path lines within the GRB study area (DSI, 2014).

(a)

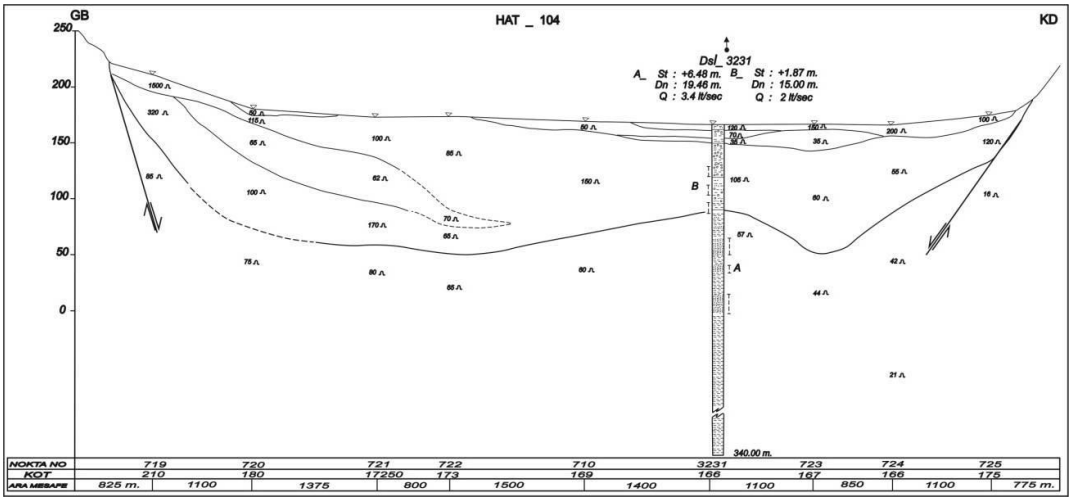

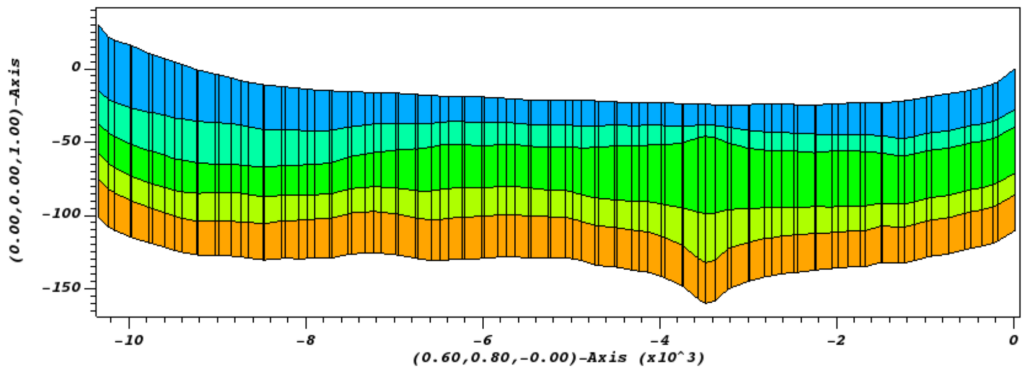

(b)

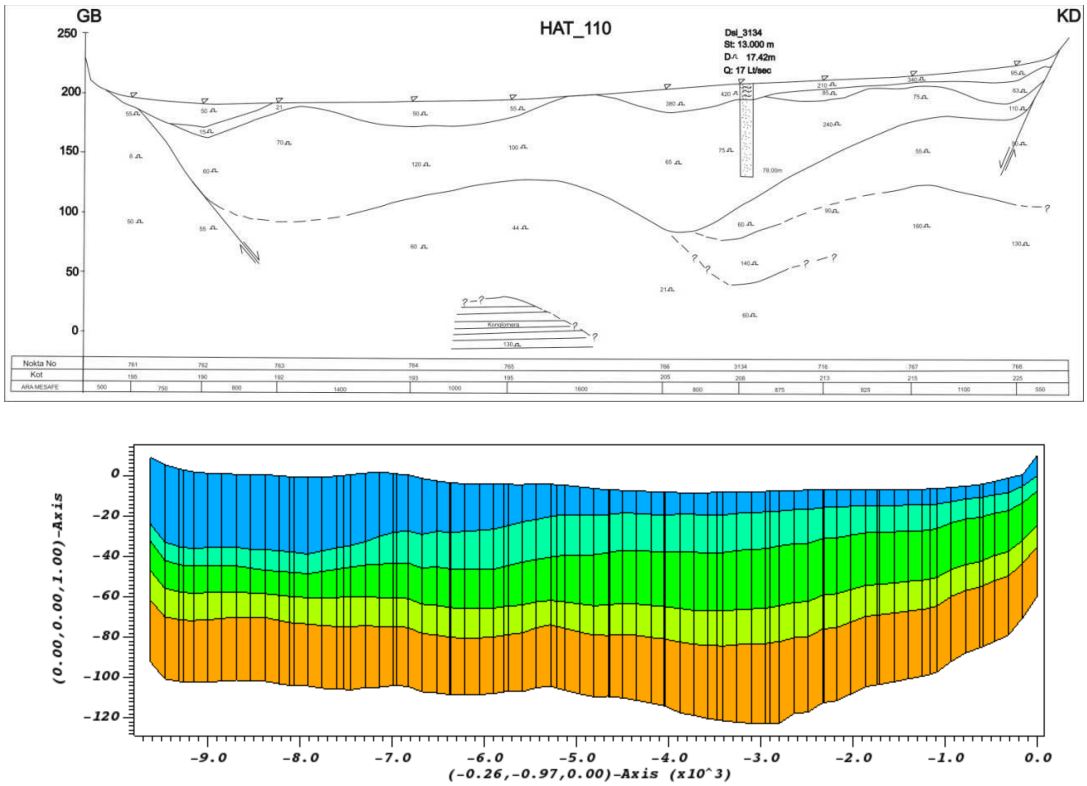

(c)

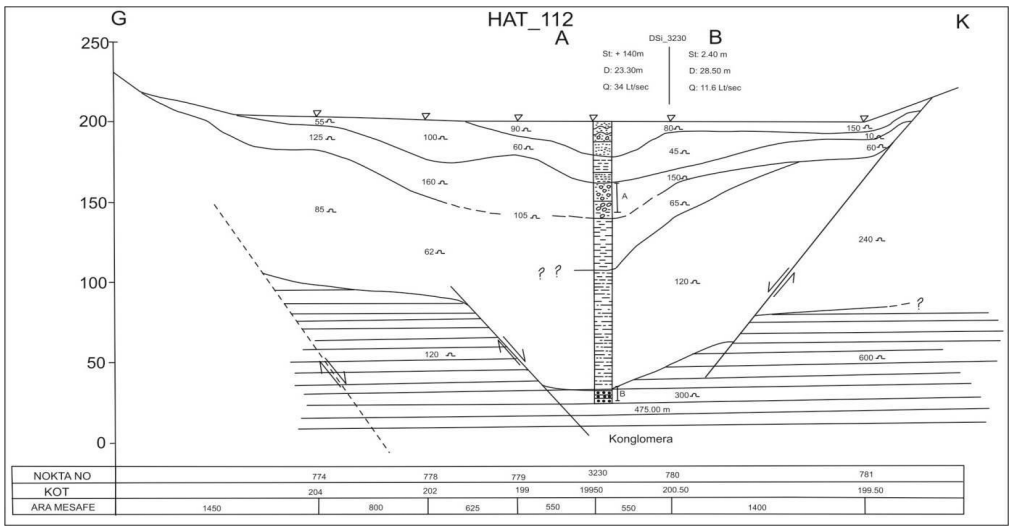

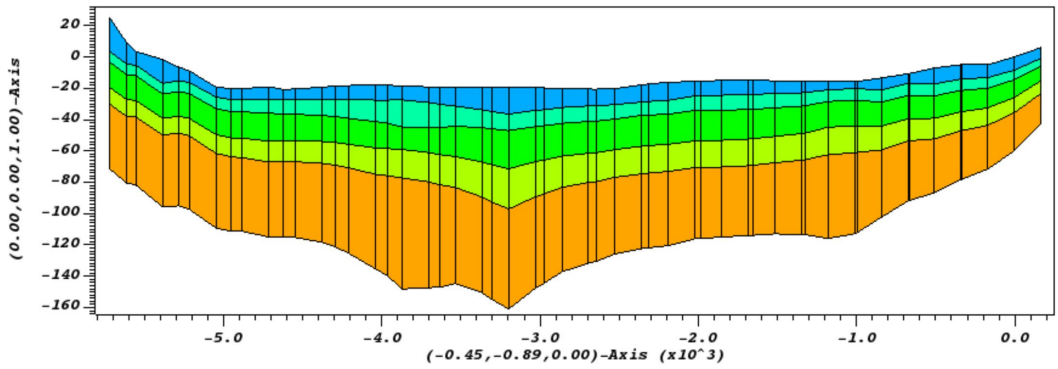

Figure 2-7 Comparisons between the geological setting of the GRB as provided by the geophysical surveys made available by DSİ (2014) and the static model developed in this study. (a) Path line 104; (b) Path line 110 and (c) Path line 112. The traces of the path lines are depicted in Figure 2-6. Only the alluvial layers (excluding the two appended layers) are presented in the subplots from the static model for a better visualization.

3 The Azraq wetland reserve, Jordan

3.1 Available geological information

The Azraq basin is a part of the limestone plateau in eastern Jordan (Figure 3-1(a)). This aquifer system can be divided into three aquifers: the upper, the middle, and the deeper aquifer. These sub-systems are hydraulically connected in a few places. As shown in Figure 3-2, the upper aquifer covers the whole basin and is comprised by four formations which are B4, B5, the Basalt (BA), and the Quaternary formation. The main units of each formation are referred to Figure 3-3. Two groups of springs in the central basin represent the main discharge outlets of the phreatic aquifer. Besides, the upper aquifer system is the main productive hydrogeologic unit, while the other two aquifer systems are relatively deep and less tapped by production wells.

The middle aquifer system is formed by B2 and A7 formations, hereinafter referred to as B2/A7. The upper aquifer system and B2/A7 are partially separated by the bituminous marl layer (B3 formation, Figure 3-3), which leads B2/A7 to be semi-confined. Part of B2/A7 outcrops in the western part of the basin. Although the average depth of B2/A7 is over hundreds of meters, more than 20 pumping wells penetrate this aquifer. Regarding the deeper aquifer system, it refers to the formations between B2/A7 and Kurnub Sandstone aquifer. Due to the poor water quality, this saline aquifer accounts for few yields. Thus, the deeper aquifer has not been considered in the groundwater flow modelling.

In addition to being the main resource of drinking water, Azraq basin also plays an important role in the environment. Azraq Oasis lies in the center of the basin (Figure 3-1(b)). It is on the list of RAMSAR Wetlands of International Importance for being the habitat for millions of migratory birds (Ramsar Convention, 1971). So far, the intensive groundwater pumping has caused the degradation of the oasis and a decrease of the groundwater stored in the aquifer system.

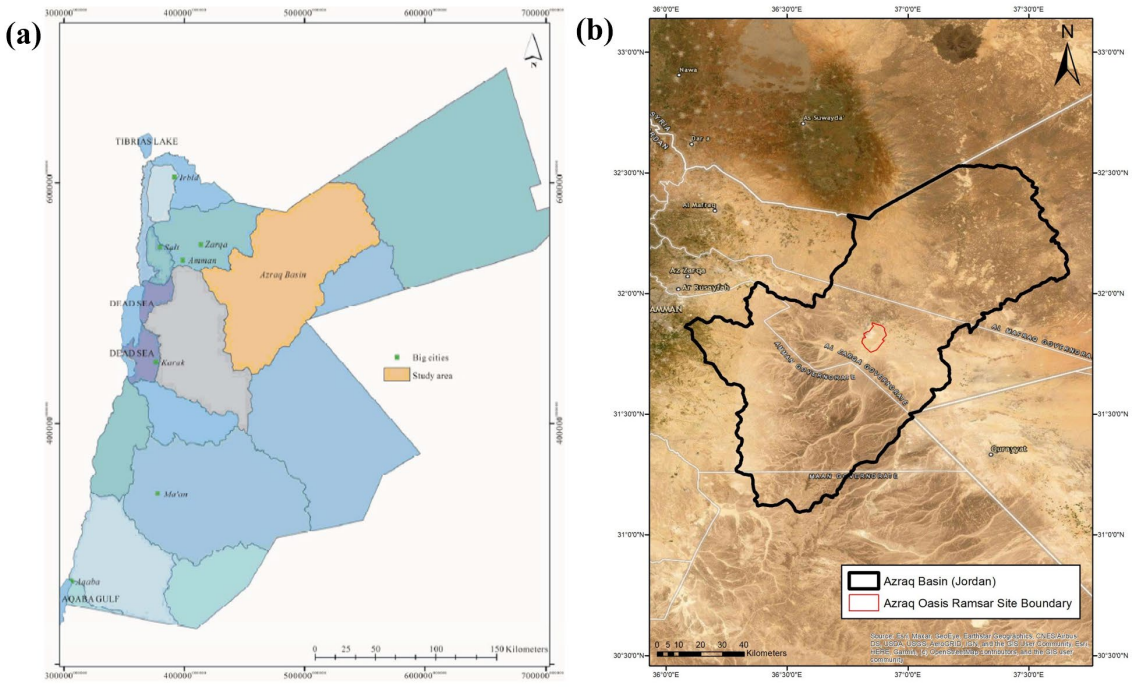

Figure 3-1 (a) Location of the selected pilot site for the Azraq basin (Alraggad and Mohammad 2010); (b) location of the Azraq Oasis.

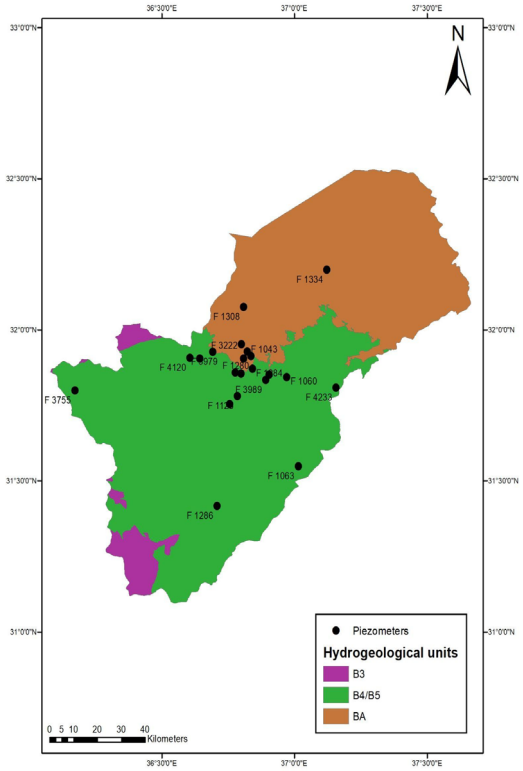

Figure 3-2 Hydrogeological units and piezometer locations in the Azraq Basin.

ERA	SYSTEM	EPOCH	GROUP	FORMATION	SYMBOL	LITHOLOGY	THICKNESS [m]	AQUIFER UNIT	
CENOZOIC	QUATERNARY	Holocene		Alluvium	Qal	clay, silt, sand, gravel		ALLUVIUM (AQUIFER) / BASALT (AQUIFER)	Upper Aquifer
		Pleistocene		Azraq	JV3	marl, clay, evaporites	20 - 150		
	TERTIARY Neogene	Pliocene			Basalt	conglomerates			
		Miocene							
		Oligocene		Qirma	JV1-2	Sandy limestone			
	TERTIARY Paleogene	Eocene	BELQA (B)	Wadi Shallala	B5	chalky and marly limestone with glauconite	0 - 550	B4/5 (AQUIFER)	
		Paleocene		Umm Rijam	B4	limestone, chalk, chert	0 - 310		
MESOZOIC	CRETACEOUS Upper	Maastrichtian		Muwaqqar	B3	chalky marl, marl, limestone chert	60 - 320	B3 (AQUITARD)	Middle Aquifer
		Campanian		Amman-Al Hisa	B2	limestone,chert, chalk, phosphorite	20 - 140	A7/B2 (AQUIFER)	
		Santonian		W.Umm Ghudran	B1	dolomitic marly limestome, marl, chert, chalk	20 - 90		
		Coniacian	AJLUN (A)	Wadi as Sir	A7	dolomitic limestone, limestone, chert, marl	60 - 340		
		Turonian		Shueib	A5/6	marl, limestone	40 - 120	A5/6 (AQUITARD)	
		Cenomanian		Hummar	A4	limestone, dolomite	30 - 100	A4 (AQUIFER)	
				Fuheis	A3	marl, limestone	30 - 90	A3 (AQUITARD)	
				Naur	A1/2	limestone, dolomite, marl	90 - 220	A1/2 (AQUIFER)	
	CRETACEOUS Lower	Albian	KURNUB (K)	Subeihi	K2	sandstone, shale	120 - 350	KURNUB (AQUIFER)	Deep Aquifer
		Aptian							
		Barremian							
		Hauterivian		Aarda	K1	sandstone, shale			
		Valanginian							
		Berriasian							

Figure 3-3 Lithological and hydrogeological classification of the aquifer systems in Azraq area (derived from Ibrahim and El-Naqa, 2018).

3.1.1 The conceptual model of aquifer system in Azraq Basin

As for GRB site, the conceptual model for Azraq basin has been presented in Deliverable 2.4. As mentioned in the last section, this conceptual model only includes the upper aquifer system and B2/A7. The B3 aquitard between upper aquifer system and B2/A7 is missing in this model since this low-permeability layer is thin and fails to span the whole study area. For the sake of simplicity, each aquifer system is conceptualized through a single layer. The corresponding isobath maps of two layers are illustrated in Figure 3-4. The basin is intercepted by several NW-SE oriented faults, where the aquifer thickness is characterized by evident jumps. The elevation of the study area is derived from a satellite-derived digital elevation model.

3.1.2 The static model of groundwater flow

The SM for groundwater model is based on the conceptual model derived in WP2. Like for the GRB site, the grid of Azraq basin is also generated by DEU through ModelMuse. The two layers are discretized into 114 rows and 98 columns. Due to the importance of the Azraq Oasis, this area is refined for a more precise characterization. The horizontal grid size varies from 500 m to 2500 m. The surroundings of Azraq basin is set to be inactive, with elements that do not join the numerical computation. The total cell number amounts to 22,344, of which 14,717 are active.

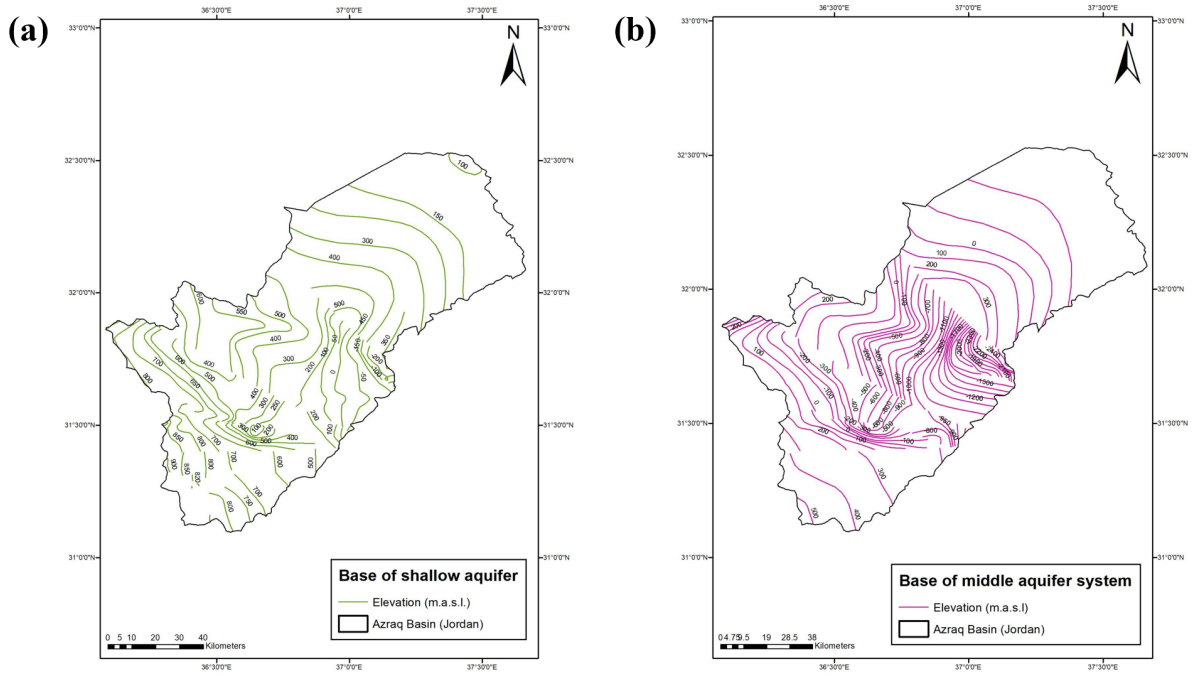

Figure 3-4 Aquifer base elevation maps for the shallow (a) and middle (b) aquifer systems in Azraq basin. The jumps of isobath lines and fault trend coincide.

3.2 Static model

3.2.1 Set up of the static model

Defining the study domain is always the first step to do be performed when it comes to the SM set-up for geomechanical modelling. The domain outline must hold the zero-displacement condition. In this case, the groundwater withdrawals mainly concentrate in the Azraq Oasis. Both drawdown and settlement in the

peripheries of the basin can be assumed to be negligible. This yields that the horizontal domain of the groundwater flow as well as the 2D discretization pattern can be maintained in the geomechanical modelling set-up.

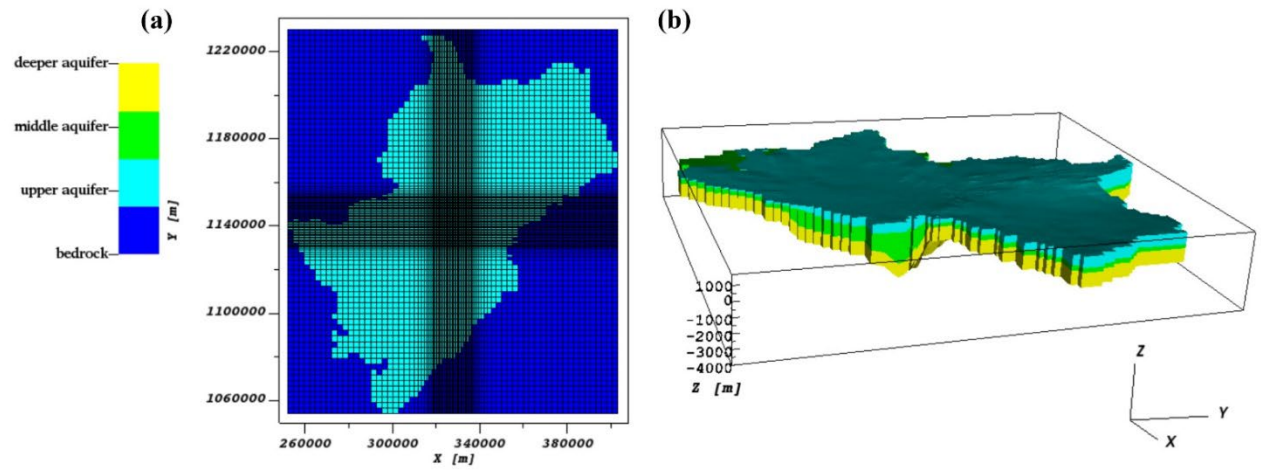

Figure 3-5 The domain of the updated SM for the Azraq Basin. (a) 2D plan view. (b) 3D perspective view. The bedrock is ruled out to focus on the aquifer system. Z axis is exaggerated by 5 times.

Vertically, the groundwater flow grid ends up with B2/A7. From the mechanical point of view, it is needed to extend the modelling domain downward until the rock to guarantee the zero-displacement criterion. Therefore, two layers are appended to the groundwater flow grid. The thickness of first appended layer is 1,000 m while the bottom of the second appended layer is fixed at -4000 m amsl. Apparently, these two layers do not represent any realistic geological layers. Instead, they are designed to be a transitional zone. The same horizontal discretization is applied to the two new layers, which consist of 114 rows and 98 columns. The final hexahedral mesh is made of 59,625 nodes and 44,688 elements (Figure 3-5).

Currently, the upper aquifer is homogeneous which may not reflect the real geological formations. However, this layer can be further subdivided into several parts with different mechanical properties. The adjustment will be dependent on the outcomes of the groundwater model.

3.2.2 Validation of the static model

As for the other pilot sites, the SM is sliced along several profiles and compared with available geologic sections. Unfortunately, only one hydrogeologic section is available in this site (Alkhatib 2017). Although the section represents a hydrogeologic sketch rather than a real geologic representation, the profile is deemed to be representative as it crosses two main faults in the study area. The comparison must be focused to the upper aquifer and B2/A7. Figure 3-6 shows the comparison, with the static model that conforms satisfactorily with the characteristics of two aquifer layers such as the basic trend and the jump caused by the faults. Due to the lack of information, the quality of the whole static model needs to be further evaluated when the outcomes of the groundwater flow model will be available.

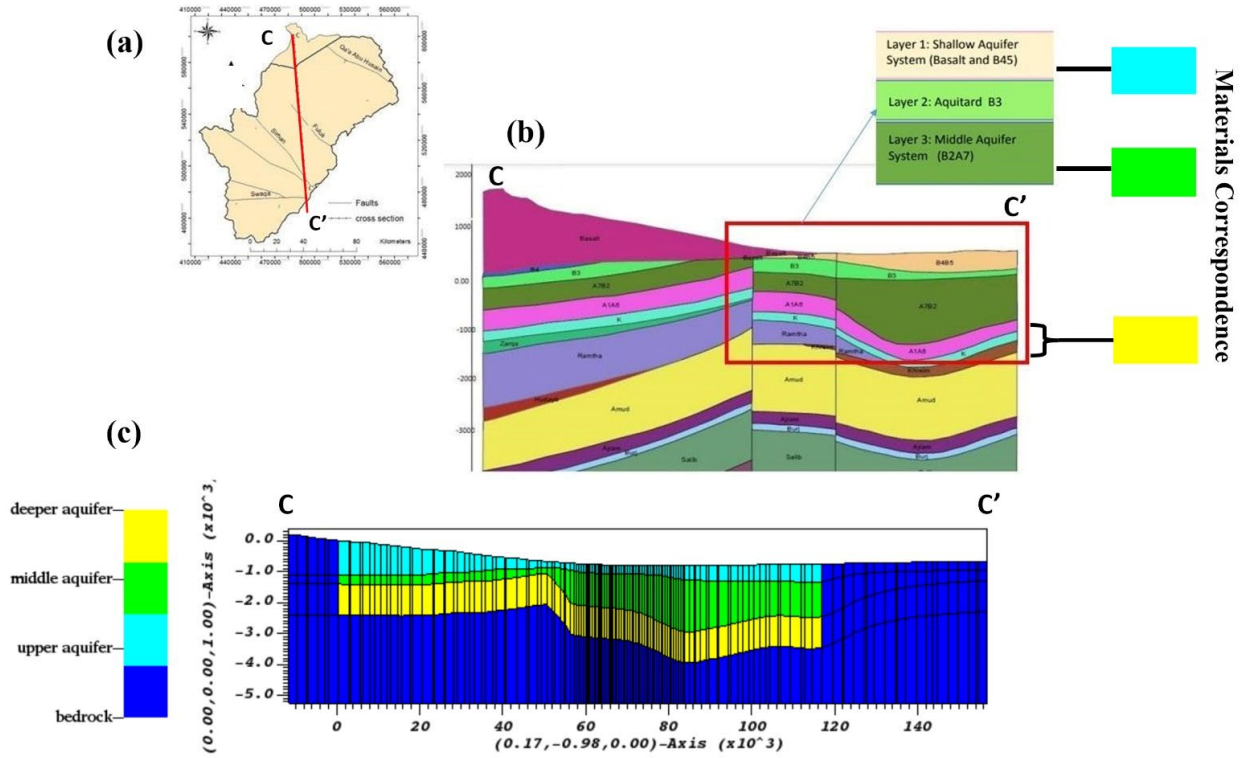

Figure 3-6 Comparison of layer profiles along the section C-C'. (a) C-C' profile location, (b) layer profile from the geological sketch after Alkhatib (2017) and (c) geomechanical model mesh along the same profile. The correspondence between the different legends is highlighted in the figure.

4 Conclusion

In this deliverable, the static models for the selected pilot sites are built-up. This work is highly related to WP5, where the static models for the groundwater flow simulations have been established. Compared to the groundwater flow model, the static model for the geomechanical simulations needs to be properly enlarged (generally both in the horizontal and vertical directions) to impose zero-displacement boundary conditions sufficiently far from the depleted aquifer system and to properly account for the mechanical effect of the bedrock (e.g., the mountain ridges). Therefore, this specific requirement makes impossible the straightforward use of the groundwater flow grids in the geomechanical model applications.

In Alto Guadalentín Basin, the northeast boundary of groundwater flow model crosses the subsidence centre. Moreover, the groundwater flow model only considers the aquifer system where the bottom of sand layers is set as an impervious boundary. Thus, we have extended horizontally the study domain to the Bajo Guadalentín Basin where InSAR data suggests no land subsidence was occurred and appended the marl and bedrock layers below the alluvial aquifer system. The Alto Guadalentín Basin is the most complicated case in terms of discretization, which is carried out through tetrahedral finite elements. The mesh is more refined (mainly along the vertical direction) than the discretization of the previous models. Moreover, each material unit is discretized with elements characterized by increasing volume according to the rank of importance. For example, the vertical size of the clay layer is around tens of meters, which allows us to depict the drawdown of the water table and the change of the saturation degree more precisely. By contrast, the size of bedrock elements is on the order of hundreds of meters, which reduces the complexity of the mesh and the CPU time.

For the Gediz River Basin and the Azraq Basin, the strategies implemented to build the static model for the geomechanical simulations are the same. The peripheries of these two areas have no significant land subsidence, so the study areas as well as 2D discretization are completely inherited from the groundwater flow model into the geomechanical model. The modifications are only along the vertical direction where we include stiff layers below the aquifer system. Due to the lack of geological information, especially at large depths, the appended layers are roughly conceptualized as uniform and homogenous layers. However, we believe such simplifications have trivial effects on the mechanical response within the aquifer system since these deeper layers generally are impervious and consolidated. At the same time, these two cases keep a hexahedral discretization totally compatible with the FD grid developed for the groundwater flow modelling. A summary of the geomechanical SM features compared to those of the groundwater flow models is provided in Table 4-1.

To verify the quality of the geomechanical static models, a few vertical sections of the mesh have been compared with available hydrogeologic profiles. The geometry of the aquifer layers are basically consistent. In conclusion, the current static models reflect satisfactorily the real hydrogeological configurations for all cases and will be used in the next phases of WP6 for the dynamic modelling.

Table 4-1 The characteristics of static models for three pilot sites.

	Alto Guadalentín Basin	**Gediz River Basin**	**Azraq Basin**
Horizontal Domain	Extended	Same	Same
Vertical Domain	Appended two layers	Appended two layers	Appended two layers
Discretization	Tetrahedra	Hexahedra	Hexahedra
Element size	Ten meters to hundreds of meters	Horizontal: 2500 m	Horizontal: 500 m to 2500 m

References

Alkhatib, Jafar. 2017. “An Integrated Approach of Analyzing Management Solutions for the Water Crisis in Azraq Basin, Jordan,” May. https://doi.org/10.53846/goediss-6311.

Alraggad, Marwan, and Alsharifa Hind Mohammad. 2010. “Managed Aquifer Recharge (MAR) through Surface Infiltration in the Azraq Basin/Jordan.” Journal of Water Resource and Protection 02 (January). https://doi.org/10.4236/jwarp.2010.212125.

Béjar-Pizarro, Marta, Carolina Guardiola-Albert, R. García-Cárdenas, Gerardo Herrera, A. Barra, A. López Molina, R.P. García-García (2016). “Interpolation of GPS and Geological Data Using InSAR Deformation Maps: Method and Application to Land Subsidence in the Alto Guadalentín Aquifer (SE Spain).” Remote Sensing 8(11). https://doi.org/10.3390/rs8110965.

Bonì, Roberta, Gerardo Herrera, Claudia Meisina, Davide Notti, Marta Béjar-Pizarro, Francesco Zucca, Pablo J. González, et al. 2015. “Twenty-Year Advanced DInSAR Analysis of Severe Land Subsidence: The Alto Guadalentín Basin (Spain) Case Study.” Engineering Geology 198 (November): 40–52. https://doi.org/10.1016/j.enggeo.2015.08.014.

Bonì, Roberta, Claudia Meisina, Pietro Teatini, Francesco Zucca, Claudia Zoccarato, Andrea Franceschini, Pablo Ezquerro, et al. (2020). "3D groundwater flow and deformation modelling of Madrid aquifer." Journal of Hydrology 585: 124773. https://doi.org/10.1016/j.jhydrol.2020.124773, 2020.

Cerón García, Juan Carlos. 1995. "Estudio hidrogeoquímico del acuífero del alto guadalentín (Murcia)." https://digibug.ugr.es/handle/10481/55814.

DSI. 2014. "Hydrogeological report for Gediz Plain." Turkey State Hydraulic Works, Izmir.

Ezquerro, Pablo, Carolina Guardiola-Albert, Gerardo Herrera, José Antonio Fernández-Merodo, Marta Béjar-Pizarro, and Roberta Bonì. 2017. "Groundwater and Subsidence Modeling Combining Geological and Multi-Satellite SAR Data over the Alto Guadalentín Aquifer (SE Spain)." Geofluids 2017: 1–17. https://doi.org/10.1155/2017/1359325.

Gambolati, Giuseppe, and Pietro Teatini. 2015. "Geomechanics of subsurface water withdrawal and injection." Water Resources Research 51: 3922-3955. https://doi.org/10.1002/2014WR016841.

Ibrahim, Khalil M., and Ali R. El-Naqa. 2018. "Inverse Geochemical Modeling of Groundwater Salinization in Azraq Basin, Jordan." Arabian Journal of Geosciences 11 (10): 237. https://doi.org/10.1007/s12517-018-3557-8.

Isotton, Giovanni, Pietro Teatini, Massimiliano Ferronato, Carlo Janna, Nicolò Spiezia, Stefano Mantica, and Giorgio Volonte'. 2019. "A robust numerical implementation of a 3D rate-dependent model for reservoir geomechanical simulations." International Journal for Numerical and Analytical Methods in Geomechanics 43: 2752-2771. https://doi.org/10.1002/nag.3000, 2019.

Nardean, Stefano, Massimiliano Ferronato, You Zhang, Shujun Ye, Xu Gong, and Pietro Teatini. 2021. "Understanding ground rupture due to groundwater overpumping by a large lab experiment and advanced numerical modelling." Water Resources Research 57: e2020WR027553. https://doi.org/10.1029/2020WR027553.

Ramsar Convention, (1971). Convention on Wetlands of International Importance especially as Waterfowl Habitat. Ramsar (Iran), UN Treaty Series No. 14583.

Seyitoglu, Gurol, Ibrahim Cemen, and Okan Tekeli. 2000. "Extensional Folding in the Alasehir (Gediz) Graben, Western Turkey." Journal of The Geological Society 157 (November): 1097–1100. https://doi.org/10.1144/jgs.157.6.1097.

Si, Hang. 2015. "TetGen, a Delaunay-Based Quality Tetrahedral Mesh Generator." ACM Transactions on Mathematical Software 41 (2): 1–36. https://doi.org/10.1145/2629697.

Sözbilir, Hasan. 2002. "Geometry and Origin of Folding in the Neogene Sediments of the Gediz Graben, Western Anatolia, Turkey." Geodinamica Acta 15 (5): 277–88. https://doi.org/10.1016/S0985-3111(02)01093-8.

Teatini, Pietro, Massimiliano Ferronato, Giuseppe Gambolati, and Marco Gonella. 2006. "Groundwater Pumping and Land Subsidence in the Emilia-Romagna Coastland, Italy: Modeling the Past Occurrence and the Future Trend." Water Resources Research 42 (1). https://doi.org/10.1029/2005WR004242.

Terzaghi, K. 1923. “Die berechnung des durchlassigkeitsziffer des tones aus dem verlauf der hydrodynamischen spannungserscheinunge.” Sitzungsber. Akad. Wiss. Wien Math. Naturwiss. Kl. 132 Abt. 2A: 125–138.

Winston, Richard B. 2019. “ModelMuse Version 4: A Graphical User Interface for MODFLOW 6.” Report 2019–5036. Scientific Investigations Report. Reston, VA. USGS Publications Warehouse. https://doi.org/10.3133/sir20195036.